Carbohydrate Research 346 (2011) 1842–1847

Contents lists available at ScienceDirect

Carbohydrate Research

journal homepage: www.elsevier.com/locate/carres

Enzymatic synthesis of novel branched sugar alcohols mediated by the transglycosylation reaction of pullulan-hydrolyzing amylase II (TVA II) cloned from *Thermoactinomyces vulgaris* R-47

Yoichiro Shimura [a,*], Keimei Oh [a], Misaki Kon [a], Eri Yamamoto [a], Yoshinori Mizuno [a], Takashi Adachi [a], Tomomi Abe [a], Shigeru Tamogami [b], Jun Fukushima [a], Tamio Inamoto [a], Takashi Tonozuka [c]

[a] Department of Biotechnology, Faculty of Bioresource Science, Akita Prefectural University, 241-438 Kaidobata-Nishi, Shimoshinjo-Nakano, Akita 010-0195, Japan
[b] Department of Biological Production, Faculty of Bioresource Science, Akita Prefectural University, 241-438 Kaidobata-Nishi, Shimoshinjo-Nakano, Akita 010-0195, Japan
[c] Department of Applied Biological Science, Faculty of Agriculture, Tokyo University of Agriculture and Technology, 3-5-8 Saiwai-cho, Fuchu, Tokyo 183-8509, Japan

ARTICLE INFO

Article history:
Received 17 March 2011
Received in revised form 14 May 2011
Accepted 27 May 2011
Available online 30 June 2011

Keywords:
Amylase
Transglycosylation reaction
Oligosaccharide
Panose
Non-reducing sugar

ABSTRACT

Transglycosylation reactions are useful for preserving a specific sugar structure during the synthesis of branched oligosaccharides. We have previously reported a panosyl unit transglycosylation reaction by pullulan-hydrolyzing amylase II (TVA II) cloned from *Thermoactinomyces vulgaris* R-47 (Tonozuka et al., *Carbohydr. Res.*, **1994**, *261*, 157–162). The acceptor specificity of the TVA II transglycosylation reaction was investigated using pullulan as the donor and sugar alcohols as the acceptor. TVA II transferred the α-panosyl unit to the C-1 hydroxyl group of *meso*-erythritol, C-1 and C-2 of xylitol, and C-1 and C-6 of D-sorbitol. TVA II differentiated between the sugar alcohols' hydroxyl groups to produce five novel non-reducing branched oligosaccharides, 1-*O*-α-panosylerythritol, 1-*O*-α-panosylxylitol, 2-*O*-α-panosylxylitol, 1-*O*-α-panosylsorbitol, and 6-*O*-α-panosylsorbitol. The Trp^{356}→Ala mutant showed similar transglycosylation reactions; however, panose production by the mutant was 4.0–4.5-fold higher than that of the wild type. This suggests that Trp^{356} is important for recognizing both water and the acceptor molecules in the transglycosylation and the hydrolysis reaction.

1. Introduction

Alpha-amylase [EC 3.2.1.1] cloned from *Thermoactinomyces vulgaris* R-47 (TVA II)[1] is a member of glycoside hydrolase family 13 (http://www.cazy.org/CAZY),[2–4] classified under subfamily 20 (GH13_20) along with neopullulanase [EC 3.2.1.125], cyclomaltodextrinase [EC 3.2.1.54] and maltogenic amylase [EC 3.1.1.133].[5] The three-dimensional structures of the GH13_20 subfamily enzymes, which have been reported for TVA II, neopullulanase from *Bacillus stearothermophilus* TRS 40, cyclomaltodextrinase from *Bacillus* sp. I-5 and *Flavobacterium* sp. No.92, and maltogenic amylase from *Thermus* species, were composed of an N-terminal domain, a catalytic $(\beta/\alpha)_8$-barrel domain, and a C-terminal domain.[6–10] These GH13_20 subfamily members differ from other typical α-amylases, such as Taka-amylase A from *Aspergillus oryzae* and cyclodextrin glucanotransferase [EC. 2.4.1.19] from *B. circulans* that do not posses the N-terminal domain.[11,12] TVA II hydrolyzes the α-(1→4) glucosidic linkage of starch, pullulan, and cyclodextrin to produce maltose, panose, and maltose, respectively. Three catalytic residues are conserved and proposed as direct catalytic residues in the GH13 amylase family of enzymes, and they were identified as Asp^{325}, Glu^{354}, and Asp^{421} in TVA II.[13,14] We proposed that these residues have an important catalytic role in TVA II, both linear and cyclic maltodextrin substrates.[15] TVA II catalyzes both hydrolysis and transglycosylation reactions. It produces two transfer products, namely, 4^2-*O*-α-isomaltosylmaltose (IMM) and 4^2-*O*-α-isomaltosylisomaltose (IMIM), using pullulan as donor and D-glucose as acceptor.[16] 2^4-*O*-α-Panosylpanose was observed in the crystal structure of TVA II saturated with panose.[17] Transglycosylation reactions as with TVA II were also reported for neopullulanase from *B. stearothermophilus* TRS40 and maltogenic amylase from *B. stearothermophilus* ET1.[18,19] Transglycosylation reactions are useful for preparing branched oligosaccharides while preserving specific structures, and have been used to produce coupling sugars, galactooligosaccharides, branched cyclodextrins, and cluster dextrins.[20–23] Trp^{356} of TVA II, positioned next to the catalytic Glu^{354} residue in conserved region 3 of the primary structure at

Abbreviations: DEPT, distortionless enhancement by polarization transfer; ESI-FT-MS, electro spray ionization Fourier transform mass spectrometry; HMQC, heteronuclear multiple quantum coherence; HPLC, high performance liquid chromatography; IMIM, 4^2-α-isomaltosylisomaltose; IMM, 4^2-α-isomaltosylmaltose; NMR, nuclear magnetic resonance; TLC, thin layer chromatography.

* Corresponding author. Tel.: +81 18 872 1574; fax: +81 18 872 1676.
E-mail address: yshimura@akita-pu.ac.jp (Y. Shimura).

0008-6215/$ - see front matter © 2011 Elsevier Ltd. All rights reserved.
doi:10.1016/j.carres.2011.05.030

the edge of the catalytic cleft, plays an important role in substrate recognition by repositioning the indole side chain during the hydrolysis reaction (Fig. 1).[13,24] The importance of this residue and its role in the transglycosylation reaction need to be studied thoroughly. We have investigated the acceptor specificity of the TVA II transglycosylation reaction and that of the Trp^{356}→Ala mutant using pullulan as donor and three sugar alcohols as acceptors. The role of Trp residues at the end of the catalytic cleft for substrate recognition in TVA II transglycosylation reactions was clarified.

2. Results and discussion

2.1. Purification of transfer products

The transfer products were analyzed by TLC and isolated by preparative HPLC. Two transfer product peaks were observed for each acceptor by HPLC; however, the TLC pattern did not follow the HPLC results for all products (Fig. 2). In the case of the *meso*-erythritol acceptor, two peaks were visible by HPLC, but only one product (E-2) could be isolated (Fig. 2A). Two products were isolated from xylitol (X-1 and X-2, Fig. 2B) and D-sorbitol (S-1 and S-2, Fig. 2C). The HPLC fractions were re-purified by preparative HPLC, and the MS spectra were then measured to determine purity and molecular mass. We finally harvested 24 mg of E-2, 69 mg of X-1, 56 mg of X-2, 27 mg of S-1, and 80 mg of S-2 from each 16 mL volumes of reaction mixture, and yields were 1.5%, 4.3%, 3.5%, 1.7%, and 5.0%, respectively. The molecular masses of E-2, X-1, X-2, S-1, and S-2 were found to be *m/z* 607.2, 637.1, 637.4, 667.1, and 667.1, respectively.

2.2. Structural analysis of transfer products

The ^1H and ^{13}C NMR, and HMQC spectra were used to identify the anomer form of the panosyl unit that was present. The panose signals at δ 5.4, 5.2, 4.9, and 4.7 ppm corresponded to the H-1^{II} (α(1→4)-linkage), the H-1^{I} α, the H-1^{III} (α(1→6)-linkage), and H-1^{I} β, respectively (Fig. 3A). No signals were observed with coupling constants of 7.0–8.0 Hz at 4.0–5.5 ppm, indicating that there were no β bonds in the transfer products (Fig. 3B–F). The new bond was expected to give a ^1H signal at about 5.0 ppm. Transfer products showed only two signals at 5.4 and 4.9 ppm in E-2, X-2, S-1, and S-2 (Fig. 3B and D–F), and the signal at 4.9 ppm had an integrated intensity of 2H, although three signals at 5.4, 5.1, and 4.9 ppm were present in X-1 (Fig. 3C). The correlation between the H-1^{I} and C-1^{I} signals in the HMQC spectra indicates an α(1→6) linkage (data not shown), and the signal at 4.9 ppm indicates a new bond, thus confirming that the α-panosyl unit was transferred to the hydroxyl group of the acceptor.

DEPT 135 spectra were used to identify the signal from the CH_2 group formed by the transglycosylation reaction (Fig. 4). For the *meso*-erythritol acceptor, a novel CH_2 signal in E-2 at 68.6 ppm differed from that of the panose and *meso*-erythritol standards (Fig. 4A–C). This result indicates that the α-panosyl unit was transferred to the C-1 position of the *meso*-erythritol acceptor; therefore, E-2 was identified as 1-*O*-α-panosylerythritol.

For the xylitol acceptor, two products were isolated by HPLC. Three transfer products were expected; 1-*O*-, 2-*O*-, or 3-*O*-α-panosylxylitol transferred an α-panosyl unit to the C-1, C-2, or C-3 hydroxyl group in xylitol, respectively. For the C-1 transfer reaction, five signals including a novel OCH_2 signal shifted by bond formation, were predicted. For the C-2, the environment of the two CH_2 groups should change considerably, and five signals for both panose and xylitol should be visible. For the C-3, only four signals should be visible because the xylitol CH_2 groups are equivalent. In the spectrum for X-1, four peaks were present, including a novel signal at 62.2 ppm, but the 60.8 ppm C-6^{II} signal from the panosyl unit disappeared (Fig. 4E). These results could indicate a C-2 position transfer reaction, because the environment of the panose C-6^{II} and the xylitol C-1 were similar and were visible as a single peak at 60.6 ppm. Five signals were visible in X-2, including the signal at 69.1 ppm (Fig. 4F), which would be consistent with a higher chemical shift of the C-1 CH_2 signal as a new OCH_2 bond was formed. The DEPT 135 and ^1H NMR results confirm X-1 as 2-*O*-α-panosylxylitol and X-2 as 1-*O*-α-panosylxylitol.

The transfer product structures for D-sorbitol were easier to predict those for xylitol. Two CH_2 signals at 62.5 and 62.9 ppm were assigned to C-1 and C-6 of D-sorbitol (Fig. 4G). In S-1, a signal appeared at 69.2 ppm while the signal at 62.5 ppm disappeared. In

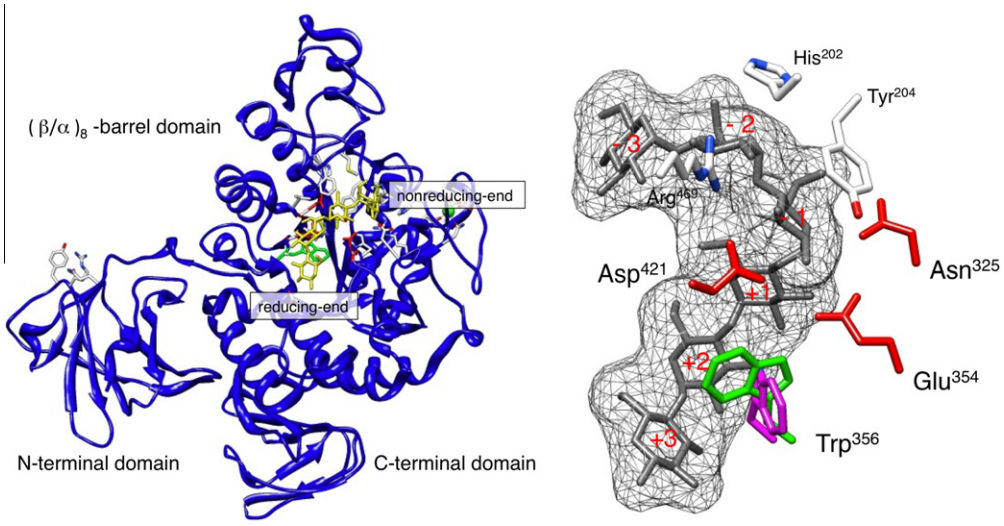

Figure 1. Model for maltohexaose binding in the catalytic cleft of TVA II. Panel A, TVA II monomer structure in the Asp^{325}→Asn mutant with maltohexaose (PDB ID: 2D2O); panel B, superimposition from lowest point in the catalytic cleft; yellow stick and gray meshed surface molecule, maltohexaose; Red residues, catalytic residues Asn^{325}, Glu^{354}, and Asp^{421}; green residue, Trp^{356} in the Asp^{325}→Asn mutants; purple residue, Trp^{356} of the wild-type TVA II; arabic numbers, subsite numbers. Substrate is hydrolyzed between subsite +1 and −1. This model was based on PDB ID: 2D2O and the purple residue on PDB ID: 1BVZ (wild type).[6,24] Molecular graphics images were produced using the UCSF Chimera package from the Resource for Biocomputing, Visualization, and Informatics at the University of California, San Francisco (supported by NIH P41 RR001081).[29]

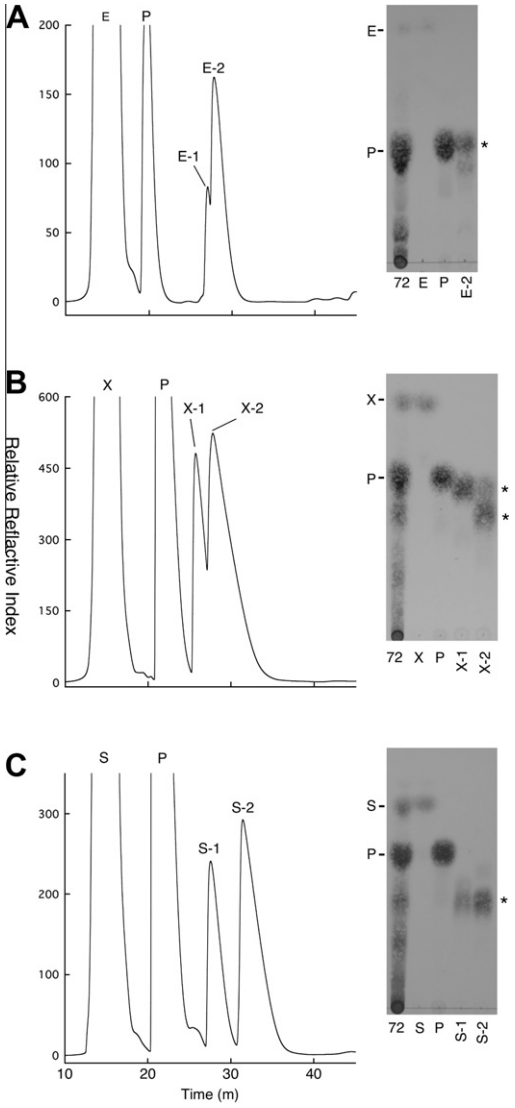

Figure 2. Chromatograms of transglycosylation products of TVA II using pullulan as donor and sugar alcohol as acceptor. Panel A, *meso*-erythritol acceptor; panel B, xylitol acceptor; panel C, D-sorbitol acceptor. Left, HPLC pattern; right, TLC pattern; 72, 72 h reaction mixture; P, panose; E, *meso*-erythritol; X, xylitol; S, D-sorbitol; asterisks, transfer products.

S-2, a signal appeared at 68.7 ppm, and the signal at 62.9 ppm disappeared. Based on these results, S-1 was identified as 1-*O*-α-panosylsorbitol, and S-2 was identified as 6-*O*-α-panosylsorbitol. Although we have previously reported an α-panosyl unit transfer reaction for glucose that gave IMM and IMIM, TVA II recognized the C-4 or C-6 of D-glucose,[16] while it did not recognize the C-4 of D-sorbitol.

2.3. Time course analysis for the transglycosylation reactions of TVA II and the Trp^{356}→Ala mutant

We were interested in the effect of amino acid substitution in the catalytic cleft not only on the hydrolysis but also on the transglycosylation reaction, because we previously found that the k_{cat}/K_m values for β-cyclodextrin and starch in the Trp^{356}→Ala mutant were decreased to 1.7% and 1.0% of wild type, respectively.[24] Therefore, time course analysis of the transfer reactions was carried out to clarify the substrate binding position within TVA II using the Trp^{356}→Ala mutant. Trp^{356} was located in the subsite +2 positioned at the edge of the catalytic cleft, close to the catalytic residue Glu^{354}.[17] TVA II and the Trp^{356}→Ala mutant showed the same HPLC trace, which suggested that substitution of Trp for Ala did not affect the binding position of donor molecule in the subsite on TVA II during the transglycosylation reaction. However, the Trp^{356}→Ala mutant showed a 4.0–4.5-fold increase in panose production compared with that of the wild type (Fig. 5). We suggest that increased panose production during the transglycosylation reaction might be caused by the stabilization of water molecules within the acceptor sugar alcohols around the catalytic cleft. Even though the Trp^{356}→Phe mutant showed about 1% of the pullulan-hydrolyzing activity of the wild type, IMM production was increased about fivefold in comparison with that of wild-type TVA II using the same pullulan-hydrolyzing unit (unpublished data). We consider that Trp^{356} is involved in two catalytic processes: one allows the donor molecules easy access to catalytic residues by indirectly producing a distortion between subsite −1 to +2; the other has to do with the acceptor molecules (Scheme 1). The Trp residue at the edge of the catalytic cleft should play an important role in both hydrolysis and transglycosylation reactions in GH13_20 subfamily enzymes and in TVA II.

3. Experimental

3.1. Generals

Pullulan (MW = 50–100 KDa) was donated by Dr. Shuzo Sakai at Hayashibara Biochemical Laboratory Inc. (Japan); *meso*-erythritol, xylitol, and D-sorbitol were purchased from Wako Pure Chemical Industries, Ltd. (Japan), and panose was purchased from MP Biomedical LLC (USA). IMM and IMIM were prepared according to a previously described method.[16] All other reagents purchased were reagent grade. Recombinant TVA II and its Trp^{356}→Ala mutant were expressed and purified from *Escherichia coli* MV1184 using previously published methods.[1,24]

3.2. Transglycosylation reaction of TVA II

The transglycosylation reaction was produced by previously described methods[16] with some minor changes; the reaction was started by adding 2 mL of enzyme solution with a pullulan-hydrolyzing activity of 1.0 unit/mL to 18 mL of a sugar solution containing 1.0 g of pullulan and 1.0 g of sugar alcohol in 0.1 M phosphate buffer (pH6.0) at 40 °C for 72 h. Aliquots (0.5 mL) of the reaction mixture were taken at 0, 0.5, 1, 2, 4, 8, 24, 48, and 72 h, and then boiled for 5 min to stop the reaction at each time point. The aliquots were applied to an analytical HPLC column for time course analysis. The approximately 16 mL of the reaction mixture remaining after the last aliquot was withdrawn and applied to a preparative HPLC column to purify the transfer products. Transfer products were monitored by TLC (Silica Gel 60 F254 plate, Merck) with 1-butanol/ethanol/water (5/5/2.5–3, v/v/v), developed using a solution of 5% sulfuric acid in methanol and charred at 150 °C.

3.3. Purification and identification of transfer products

3.3.1. Preparation and purification of transfer products

Time course samples were analyzed by HPLC (Mightysil RP-18 GP Aqua column φ 4.5 × 250 mm; Kanto Chemical Co. Inc., Japan) with Milli-Q water at a flow rate of 0.8 mL/min at 40 °C, and quantified as the D-glucose equivalent. Transfer products from each 72 h reaction mixtures were purified by preparative HPLC (Mightysil RP-18 GP Aqua column, φ 20 × 250 mm; Kanto Chemical Co. Inc., Japan) with Milli-Q water at a flow rate of 4.0 mL/min at room temperature and detected by a refractive index (RI) detector (Hitachi L-7490; Japan).

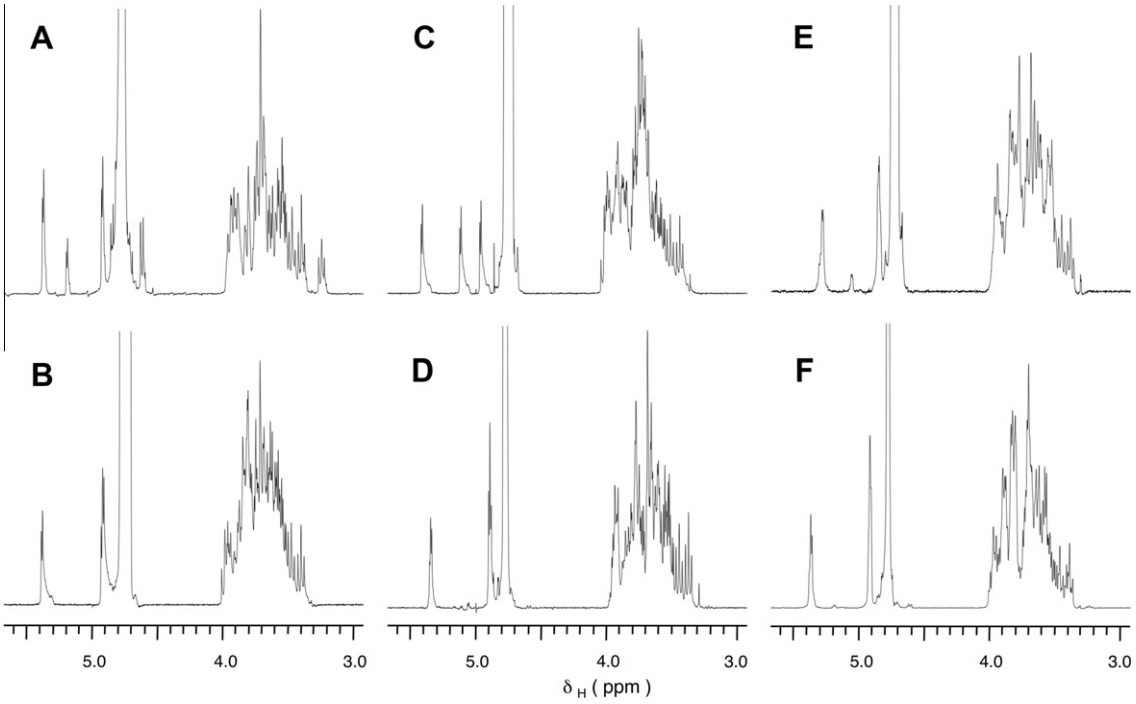

Figure 3. Comparison of ^{1}H NMR spectra of the transfer products of the TVA II transglycosylation reaction. Panel A, panose; panel B, E-2; panel C, X-1; panel D, X-2; panel E, S-1; panel F, S-2. ^{1}H NMR spectra were measured in D_2O on a JMN-400 FT-NMR system.

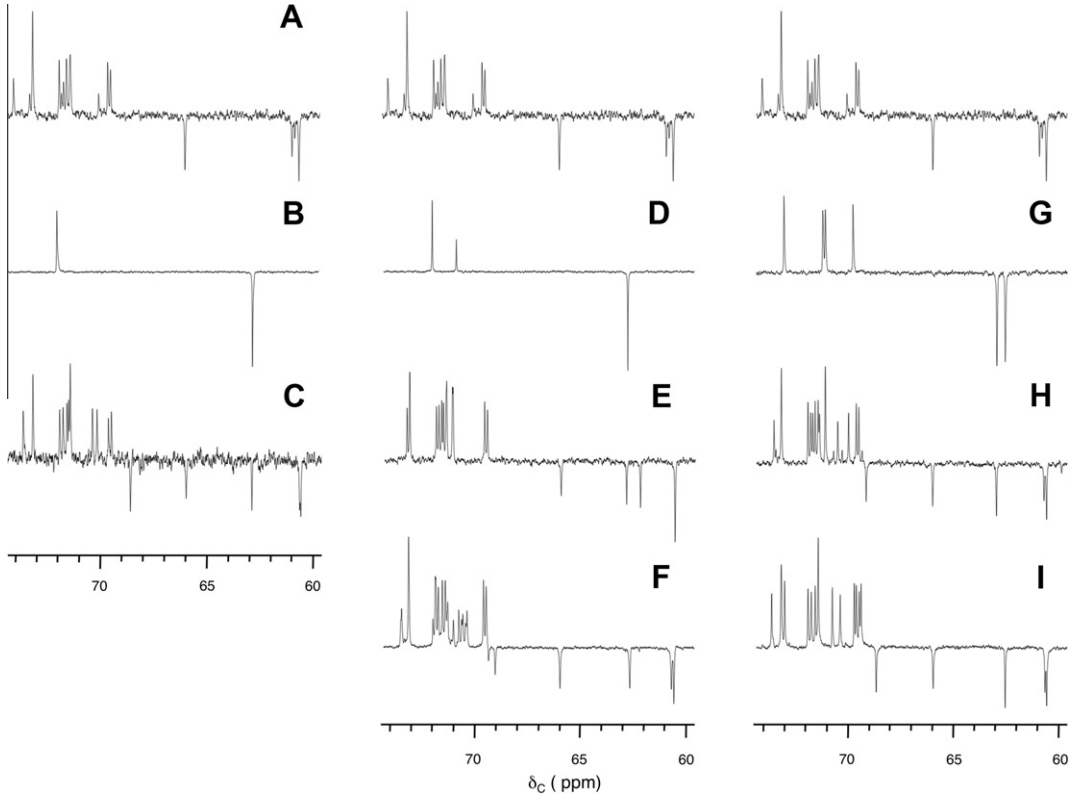

Figure 4. Comparison of DEPT 135 spectra of the TVA II transglycosylation reaction transfer products. Panel A, panose; panel B, *meso*-erythritol; panel C, E-2; panel D, xylitol; panel E, X-1; panel F, X-2; panel G, D-sorbitol; panel H, S-1; panel I, S-2. DEPT 135 spectra were measured in D_2O on a JMN-400 FT-NMR system.

The purity and molecular mass (*m/z*) of the transfer products were analyzed on a TSQ Quantum Ultra ESI-FT-MS system (Thermo Fisher Scientific, USA) in negative ion mode. A sample of about 1 mg/mL in 80% methanol was injected directly by syringe. The MS/MS spectrum was measured in negative ion mode with product ion scan analysis (collision energy 15–25 eV). The main transfer

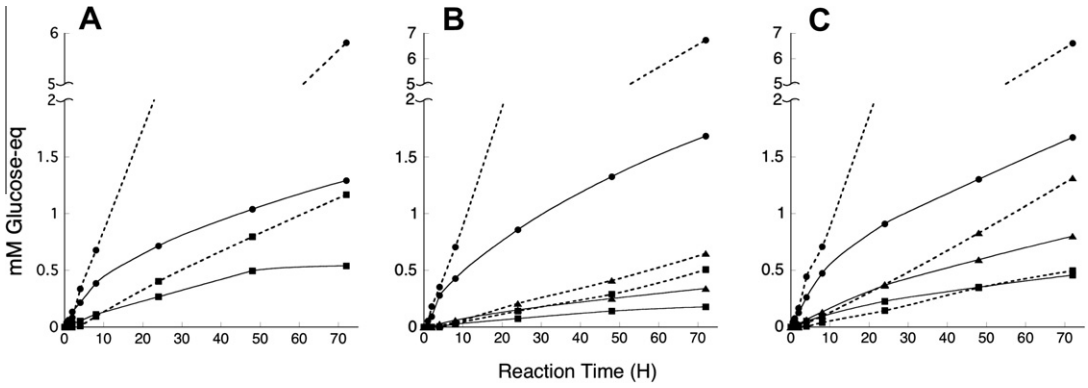

Figure 5. Time course analysis of transglycosylation reactions of wild-type TVA II and its Trp^{356}→Ala mutant. Time course fractions quantified by analytical HPLC as the glucose equivalent. Panel A, *meso*-erythritol acceptor; panel B, xylitol acceptor; panel C, D-sorbitol acceptor. Solid line, wild type TVA II; dashed line, Trp^{356}→Ala mutant; ●, panose; ■, X-1 or S-1; ▲, E-1 + E-2, X-2, or S-2.

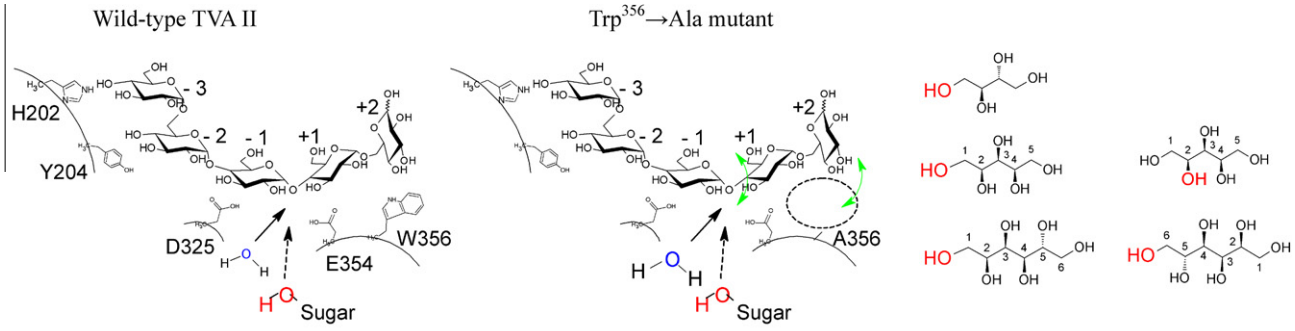

Scheme 1. Transglycosylation reaction of TVA II cloned from *T. vulgaris* R-47 with pullulan as the donor and sugar alcohol as the acceptor. Trp^{356} contribute to substrate binding on catalytic cleft, especially, subsite +2, in hydrolysis and transglycosylation reaction.

products and the co-fragment pattern of panose, IMM, and IMIM were checked against data reported by Usui et al.[25]

^{1}H and ^{13}C NMR, DEPT 135, and HMQC spectra for a 10 mg/mL sample in deuterium oxide (D_2O, 99.8 atm %; Acros Organics, USA) were measured on a JNM-EPC400 FT-NMR system (400 MHz; JEOL, Japan) in auto solvent mode. The spectra of transfer products were compared with those of panose and acceptors, as well as reference data.[26–28]

3.3.2. Identification of transfer products

3.3.2.1. 1-*O*-α-Panosylerythritol (E-2). ^{1}H NMR: δ 5.39 (d, 1H, J = 4.0 Hz, H-1^{II}), 4.91 (t, 2H, J = 4.0 Hz, H-1^{III}, 1^{I} α). ^{13}C NMR: δ 99.9 (CH, C-1^{II}), 98.2 (CH, C-1^{III}), 98.1 (CH, C-1^{I}), 77.2, 73.7, 73.2 (2C's), 71.9, 71.8, 71.6, 71.5, 71.4 (2C's), 70.4, 70.2, 69.6, 69.5, 68.6 (CH_2, C-1^{E}), 66.0 (CH_2, C-6^{II}), 62.9 (CH_2, C-4^{E}), 60.6 (2C's, CH_2, C-6^{I}, 6^{III}). ESI-MS (negative): calcd for $C_{22}H_{39}O_{19}$ $[M-H]^-$: 607.54; found, *m/z* 607.21.

3.3.2.2. 2-*O*-α-Panosylxylitol (X-1). ^{1}H NMR: δ 5.41 (d, 1H, J = 4.0 Hz, H-1^{II}), 5.12 (d, 1H, J = 4.0 Hz, H-1^{I} α), 4.96 (d, 1H, J = 4.0 Hz, H-1^{III}). ^{13}C NMR: δ 100.2 (CH, C-1^{I}), 100.0 (CH, C-1^{II}), 98.2 (CH, C-1^{III}), 80.2, 77.2, 73.3, 73.2 (2C's), 71.8, 71.7, 71.6, 71.4 (2C's), 71.2, 71.1, 69.6, 69.5, 66.0 (CH_2, C-6^{II}), 62.9 (CH_2, C-5^{X}), 62.2 (CH_2, C-1^{X}), 60.6 (2C's, CH_2, C-6^{I}, 6^{III}). ESI-MS (negative): calcd for $C_{23}H_{41}O_{20}$ $[M-H]^-$: 637.57; found, *m/z* 637.10.

3.3.2.3. 1-*O*-α-Panosylxylitol (X-2). ^{1}H NMR: δ 5.37 (d, 1H, J = 3.7 Hz, H-1^{II}), 4.91 (t, 2H, J = 4.0 Hz, H-1^{III}, 1^{I} α). ^{13}C NMR; δ 99.9 (CH, C-1^{II}), 98.4 (CH, C-1^{I}), 98.2 (CH, C-1^{III}), 77.3, 73.5, 73.2 (2C's), 71.9 (2C's), 71.8, 71.6, 71.4, 71.3, 70.8, 70.6, 70.4, 69.6, 69.5, 69.1 (CH_2, C-5^{X}), 66.0 (CH_2, C-6^{II}), 62.7 (CH_2, C-1^{X}), 60.7 (CH_2, C-6^{I}), 60.6 (CH_2, C-6^{III}). ESI-MS (negative): calcd for $C_{23}H_{41}O_{20}$ $[M-H]^-$: 637.57; found, *m/z* 637.44.

3.3.2.4. 1-*O*-α-Panosylsorbitol (S-1). ^{1}H NMR: δ 5.35 (d, 1H, J = 4.0 Hz, H-1^{II}), 4.91 (t, 2H, J = 4.0 Hz, H-1^{III}, 1^{I} α). ^{13}C NMR; δ 99.8 (CH, C-1^{II}), 98.1 (CH, C-1^{II}), 97.9(CH, C-1^{III}), 77.4, 73.5, 73.2 (2C's), 71.9, 71.8, 71.7, 71.6, 71.4, 71.3, 71.1 (2C's), 70.5, 70.0, 69.6, 69.5, 69.2 (CH_2, C-1^{S}), 66.0 (CH_2, C-6^{II}), 63.0 (CH_2, C-6^{S}), 60.7 (CH_2, C-6^{I}), 60.6 (CH_2, C-6^{III}). ESI-MS (negative): calcd for $C_{24}H_{43}O_{21}$ $[M-H]^-$: 667.59; found, *m/z* 667.12.

3.3.2.5. 6-*O*-α-Panosylsorbitol (S-2). ^{1}H NMR: δ 5.36 (d, 1H, J = 4.0 Hz, H-1^{II}), 4.91 (t, 2H, J = 4.0 Hz, H-1^{III}, 1^{I} α). ^{13}C NMR; δ 99.8 (CH, C-1^{II}), 98.1 (CH, C-1^{II}), 98.0 (CH, C-1^{III}), 77.3, 73.7, 73.2 (2C's), 73.0, 71.9, 71.8, 71.6, 71.4 (2C's), 70.8, 70.4, 69.7, 69.6, 69.5, 69.4, 68.7 (CH_2, C-6^{S}), 66.0 (CH_2, C-6^{II}), 62.5 (CH_2, C-1^{S}), 60.7 (CH_2, C-6^{I}), 60.6 (CH_2, C-6^{III}). ESI-MS (negative): calcd for $C_{24}H_{43}O_{21}$ $[M-H]^-$: 667.59; found, *m/z* 667.13.

3.3.2.6. Standard materials. *meso*-Erythritol: ^{13}C NMR; δ 62.7 (CH_2, C-1^{E}, 4^{E}), 72.0 (CH, C-2^{E}, 3^{E}).

Xylitol: ^{13}C NMR; δ 62.7 (CH_2, C-1^{X}, 5^{X}), 70.9 (CH, C-3^{X}), 72.0 (CH, C-2^{X}, 4^{X}).

D-Sorbitol: ^{13}C NMR; δ 62.5 (CH_2, C-1^{S}), 62.9 (CH_2, C-6^{S}), 69.7 (CH, C-3^{S}), 71.1 (CH, C-5^{S}), 71.2 (CH, C-4^{S}), 73.0 (CH, C-2^{S}).

Panose: ^{1}H NMR; δ 5.38 (d, 1H, J = 4.1 Hz, H-1^{II}), 5.20 (d, 0.4H, J = 4.0 Hz, H-1^{I} α), 4.93 (d, 1H, J = 3.6, H-1^{III}), 4.62 (d, 0.6H, J = 7.7, H-1^{I} β). ^{13}C NMR; δ 99.8 (CH, C-1^{II}), 98.2 (CH, C-1^{III}), 95.9 (CH, C-1^{I} β), 92.0 (CH, C-1^{I} α), 77.4, 77.2, 76.3, 74.7, 74.1, 73.3, 73.2

(2C's), 71.9, 71.8, 71.7, 71.6, 71.4, 70.1, 69.7, 69.5, 66.0 (CH_2, C-6^{II}), 60.9 (CH_2, C-6^{I} β), 60.7 (CH_2, C-6^{I} α), 60.5 (CH_2, C-6^{III}). ESI-MS (negative): calcd for $C_{18}H_{31}O_{16}$ $[M-H]^-$: 503.44; found, *m/z* 503.05.

Acknowledgments

We thank Dr. Shuzo Sakai at Hayashibara Biochemical Laboratory Inc. for donating pullulan and Dr. Yoshiyuki Sakano Professor Emeritus at Tokyo University of Agriculture and Technology for advice. We wish to thank Common Instruments Center, Faculty of Bioresource Sciences, Akita Prefectural University, for NMR and mass measurement. This work was partially supported by a Grant-in-Aid for Scientific Research (#18780076, Y.S.) from The Ministry of Education, Culture, Sports, Science and Technology (MEXT) of Japan.

References

1. Tonozuka, T.; Ohtsuka, M.; Mogi, S.; Sakai, H.; Ohta, T.; Sakano, Y. *Biosci. Biotech. Biochem.* **1993**, *57*, 395–401.
2. Henrissat, B. *Biochem. J.* **1991**, *280*, 309–316.
3. Henrissat, B.; Bairoch, A. *Biochem. J.* **1993**, *293*, 781–788.
4. Henrissat, B.; Bairoch, A. *Biochem. J.* **1996**, *316*, 695–696.
5. Stam, M. R.; Danchin, E. G. J.; Rancurel, C.; Coutinha, P. M.; Henrissat, B. *Protein Eng., Des. Sel.* **2006**, *19*, 555–562.
6. Kamitori, S.; Kondo, S.; Okuyama, K.; Yokota, T.; Shimura, Y.; Tonozuka, T.; Sakano, Y. *J. Mol. Biol.* **1999**, *287*, 907–921.
7. Hondoh, H.; Kuriki, T.; Matsuura, Y. *J. Mol. Biol.* **2003**, *326*, 177–188.
8. Lee, H.-H.; Kim, M.-S.; Cho, H.-S.; Kim, J.-I.; Kim, T.-J.; Choi, J.-H.; Park, C.; Lee, H.-S.; Oh, B.-H.; Park, K.-H. *J. Biol. Chem.* **2002**, *277*, 21891–21897.
9. Kim, J.-S.; Cha, S.-S.; Kim, H.-J.; Kim, T.-J.; Ha, N.-C.; Oh, S.-T.; Cho, H.-S.; Cho, M.-J.; Kim, M.-J.; Lee, H.-S.; Kim, J.-W.; Choi, K. Y.; Park, K.-H.; Oh, B.-H. *J. Biol. Chem.* **1999**, *274*, 26279–26286.
10. Fritzsche, H.; Schwede, T.; Schulz, G. E. *Eur. J. Biochem.* **2003**, *270*, 2332–2341.
11. Matsuura, Y.; Kusunoki, M.; Harada, W.; Kakudo, M. *J. Biochem.* **1984**, *95*, 697–702.
12. Klein, C.; Schulz, G. E. *J. Mol. Biol.* **1991**, *217*, 737–750.
13. Nakajima, R.; Imanaka, T.; Aiba, S. *Appl. Microbiol. Biotechnol.* **1986**, *23*, 355–360.
14. Ichikawa, K.; Tonozuka, T.; Yokota, T.; Shimura, Y.; Sakano, Y. *Biosci. Biotechnol. Biochem.* **2000**, *64*, 2692–2698.
15. Ohtaki, A.; Mizuno, M.; Tonozuka, T.; Sakano, Y.; Kamitori, S. *J. Biol. Chem.* **2004**, *279*, 31033–31040.
16. Tonozuka, T.; Sakai, H.; Ohta, T.; Sakano, Y. *Carbohydr. Res.* **1994**, *261*, 157–162.
17. Mizuno, M.; Tonozuka, T.; Uechi, A.; Ichikawa, K.; Kamitori, S.; Nishikawa, A.; Sakano, Y. *Eur. J. Biochem.* **2004**, *271*, 2530–2538.
18. Takata, H.; Kuriki, T.; Okada, S.; Takesada, Y.; Iizuka, M.; Minamiura, N.; Imanaka, T. *J. Biol. Chem.* **1992**, *267*, 18447–18452.
19. Cha, H.-J.; Yoon, H.-G.; Kim, Y.-W.; Lee, H.-S.; Kim, J.-W.; Kweon, K.-S.; Oh, B.-H.; Park, K.-H. *Eur. J. Biochem.* **1998**, *253*, 251–262.
20. Okada, S.; Kitahata, S. *Nippon Shokuhinkogyo Kaishi* **1975**, *22*, 420–424.
21. Mozaffer, Z.; Nakanishi, K.; Matsuno, R.; Kamikubo, T. *Agric. Biol. Chem.* **1984**, *48*, 3053–3061.
22. Sumaya, K.; Adachi, S.; Sohma, T.; Itoh, T. *Agric. Biol. Chem.* **1986**, *50*, 2069–2075.
23. Takata, H.; Ohdan, K.; Takaha, T.; Kuriki, T.; Okada, S. *J. Appl. Glycosci.* **2003**, *50*, 15–20.
24. Ohtaki, A.; Mizuno, M.; Yoshida, H.; Tonozuka, T.; Sakano, Y.; Kamitori, S. *Carbohydr. Res.* **2006**, *341*, 1041–1046.
25. Usui, T.; Ogata, M.; Murata, T.; Ichikawa, K.; Sakano, Y.; Nakamura, Y. *J. Carbohydr. Chem.* **2009**, *28*, 421–430.
26. Usui, T.; Yokoyama, M.; Yamaoka, N.; Matsuda, K.; Tuzimura, K.; Sugiyama, H.; Seto, S. *Carbohydr. Res.* **1974**, *33*, 105–116.
27. Usui, T.; Yamaoka, N.; Matsuda, K.; Tuzimura, K.; Sugiyama, H.; Seto, S. *J. Chem. Soc., Perkin Trans. 1* **1973**, 2425–2432.
28. Spectral Database for Organic Compounds SDBS (SDBSWeb): http://riodb01.ibase.aist.go.jp/sdbs/ (National Institute of Advanced Industrial Science and Technology, Japan).
29. Pettersen, E. F.; Goddard, T. D.; Huang, C. C.; Couch, G. S.; Greenblatt, D. M.; Meng, E. C.; Ferrin, T. E. *J. Comput. Chem.* **2004**, *25*, 1605–1612.